The Principle and State-of-Art Approach for Black Hole Detection

Lingyan Guan[1, a†], Xianzhe Tang[2, †], Jialing Tian[3, *†], Jiayi Wu[4, c†]

[1]Department of Physics, University of Strathclyde, Glasgow, United Kingdom

[2]Department of Physics and Astronomy, Stony Brook University, Stony Brook, NY, USA

[3]Department of Physics and Astronomy, The University of Manchester,Manchester, United Kingdom

[4] Department of Physics, Sichuan University, Chengdu, China

[a]lingyan.guan.2021@uni.strath.ac.uk; [b] xianzhe.tang@stonybrook.edu; [c]wujiayi777@stu.scu.edu.cn

*Corresponding author: jialing.tian@student.manchester.ac.uk;

[†]These authors contributed equally

Abstract—Black hole is a kind of special celestial subject whose density is so great that even the light cannot escape, which has always been a popular topic. This study will present the recent progress of observation related to three quantities of black holes. As a leading-in, we first introduced some of the most commonly discussed black holes by demonstrating their field equations, metric, and some other representative quantities. On this basis, the formation process of a black hole will be described. In addition, a picture of the detectors used in cosmology observation is discussed before getting any further into the methods applied in observation. Subsequently, we summarized observations regarding the three elements of a black hole (mass, charge and spin). For these three different characters of black hole, different methods and theories were put into use, including gravitational retro-lensing, twin-peak QPOs, accretion disks, continuum fitting method, and black body radiation. Eventually, possible limitations are evaluated and possible improving approaches on current observations are proposed. Overall, these results shed light on guiding further researches focusing on exploring the black holes.

1. INTRODUCTION

In general, black hole refers to the areas with extremely large density, it creates great gravitation potential, where no particles or electromagnetic can escape from their powerful tug of gravity. If matters (e.g., stars, planets, or spacecrafts) get too close, they will be stretched and compressed [1]. Black holes can be classified by three different properties: mass, charge and spin. According to the general relativity proposed by Einstein, the black holes ought to be existed in the universe, while the term is coined in 1967 by Wheeler [2]. In retrospect, the first possible discovery of the black holes was achieved in 1971, while the Interferometer Gravitational-Wave Observatory (LIGO) detected gravitational wave of the black holes merging in 2015 remarks key steps for further exploration of the black holes [2].

Black holes have been an intriguing topic ever since Einstein predicted their existence, people have gone from solving black hole solutions to attempting at observing relative phenomena. The essential

feature of black holes that it could absorb even the light makes it a rather uneasy task to observe them, yet researchers were never hampered by this, they study phenomena specialized to black hole and made efforts trying to take use of these phenomena to show that black holes do exist. According to the observations, existence of black holes can be proved, meanwhile a better understanding of their properties can be gained. Actually, scholars have been reaching out for aspects including the three properties of black holes, namely mass, charge and the spin.

Researches on black hole are meaningful. Firstly, BH is a secret topic within the field of astrophysics, because it is hard to observe black hole with our eyes or simple equipment, also it cannot reflect any light, and there might be some special matters within the black hole. Meanwhile, there are lots of special matters in black holes, hence it is useful to get more information about it. Because of black holes, many objects and mater around them will be affect, it is a meaningful field to do researches and use these discusses to help other aspects in astronomy. The rest part of the paper is organized as follows. Sec. II will discuss basic descriptions of black holes. Sec. III will present several kinds of black holes. The Sec. VI will discuss the detection of three parameters black hole.

2. BASIC DESCRIPTIONS OF BLACK HOLES

Black hole is an astronomical body with a great gravitation, where the spacetime around curved so much that even light can't escape from it. On this basis, the boundary of the black holes is what we call event horizon, because no information can be sent out through the event horizon since the strong gravity. For a non-rotate black hole, the basic equation of the event horizon can be described as:

$$r_S = \frac{2GM}{c^2} \tag{1}$$

Here, G is gravitational constant, M is the mass of the black hole, c is the speed of light. However, almost all the black holes in the universe can be seen as rotating black hole, since nearly all the astronomical object that black holes generated from has a rotate spin. Furthermore, the collide of black holes and other astronomical body can generate angular momentum in black hole. In the theoretical research, a non-dimensional parameter a is often given relating to the spin. It's relation with mass and angular momentum can be determined as:

$$a = \frac{cJ}{GM^2} \tag{2}$$

Here, a is the non-dimensional parameter and J is the angular momentum of the black hole. For a rotating black hole, as shown in Fig. 1, the event horizon can be determined as [3]**:**

$$\text{Outer event horizon}: \quad r_+ = m + \sqrt{m^2 - a^2} \tag{3}$$

$$\text{Inner event horizon}: \quad r_- = m - \sqrt{m^2 - a^2} \tag{4}$$

For a rotating black holes, the singularity will become a ring, which can be describe as $r = a$,

$$\begin{cases} x^2 + y^2 = a^2 \\ z = 0 \end{cases} \tag{5}$$

As a matter of fact, there are three quantities can be determined for a black hole, which are mass, electric charge and the spin. The value of the mass of a black hole has a wide range. For a supermassive black hole (e.g., Sgr A* in Fig.2), it can hold a mass about 0.1 million $M_{\odot}$. The primordial black holes generated soon after the big bang is thought to has 10^{-5}g at minimum [4]**.**

The electric charge for an astronomical black hole is likely far less than its theoretical maximum [6]. The universe is generally electrically neural; hence, the materials create the black holes and intake by the black holes usually will not take large electric. Therefore, black holes are not predicted to bring that extreme number of electric charges. Moreover, the reason that the electromagnetic repulsion is far larger than average gravitational force gives another strong certification of it.

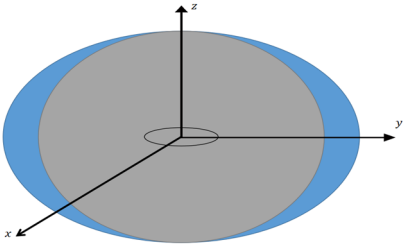

Figure 1. The inner and outer event horizon of the rotating Kerr black hole. The circular inside is the ring singularity

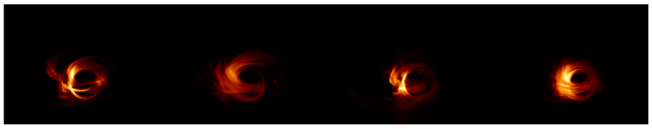

Figure 2. Predicted image of the Sgr A* Image credit [5].

3. CATEGORY OF BLACK HOLES

In general, we focus on 4 types of black holes: Schwarzschild, Reissner-Nordström, Kerr and Kerr-Newman black hole. The Schwarzschild geometry can be described as:

$$ds^2 = -\left(1 - \frac{2M}{r}\right)dt^2 + \left(1 - \frac{2M}{r}\right)^{-1} dr^2 + r^2 d\Omega_2{}^2 \tag{6}$$

where s is Schwarzschild metric, $0 < r < \infty$ is a radial coordinate, t is the time coordinate, and Ω is a point on the two spheres s^2, $d\Omega_2{}^2 = d\theta^2 + \sin^2\theta d\phi^2$ is the round metric on the two-sphere. From the Schwarzschild' geometry above, the least connected, massless scalar fields represent a spherically symmetric collapse. This solution depicts the generation of naked singularities and black holes depending on the values of specific parameters. Because black holes are known as Schwarzschild black holes, it's only reasonable to wonder how these black holes form when scalar fields collapse. Due to the mass M, the gravitation of a particle will become time independent at a point in the space. Fig. 3 gives a sketch of Schwarzschild black hole and the radial and angular direction in the Schwarzschild solution.

The escape velocity of the Schwarzschild black hole is equal to the velocity of light, which is:

$$v = \sqrt{\frac{2GM}{R}} \tag{7}$$

Where v is the escape velocity of a Schwarzschild black hole, G is the Newton's gravitational constant, M is the mass, and R is the radius. Three classical representations of the Schwarzschild metric are given in Table. 1. The Schwarzschild metric is represented in six different ways as summarized in Table. 2.

With regard to the Reissner-Nordström (RN) black hole, it is a kind of charged non-rotating black hole with no angular momentum, which has geometry of according to Ref. [8]:

$$ds^2 = -\left(1 - \frac{2M}{r} + \frac{Q^2}{r^2}\right)dt^2 + \left(1 - \frac{2M}{r} + \frac{Q^2}{r^2}\right)^{-1} dr^2 + r^2(d\theta^2 + sin^2\theta d\phi^2) \tag{8}$$

Here,

$$\mathrm{M} = \frac{Gm}{c^2} \tag{9}$$

$$Q^2 = \frac{q^2 G}{4\pi\varepsilon_0 c^4} \tag{10}$$

where q is the charge, ε_0 is the electric constant and the radii can be described as:

$$r_{\pm} = M \pm \sqrt{M^2 - Q^2} \tag{11}$$

As for Kerr black hole**,** the geometry can be written as

$$dr^2 = \left(1 - \frac{2M}{r}\right)dt^2 + \frac{4Ma}{r}dtd\phi - \frac{dr^2}{1 - \frac{2M}{r} + \frac{a^2}{r^2}} - \left(1 + \frac{a^2}{r^2} + \frac{2Ma^2}{r^3}\right)r^2 d\phi^2 \tag{12}$$

where r is a radial coordinate, J is the angular momentum of the black hole, a=J/M which also called Kerr parameter. Fig. 4 shows the structure of Kerr black hole. The three classical representations of the Kerr metric are listed in Table. 3.

A representation of the multiple horizons' spatial appearances and relationships, as well as the Kerr metric's singularity These are, expressively, from the outside to the inside (Seen from the Table. 4). Inner ergosurface and Cauchy horizon disappear at a = 0, while outer ergosurface and event horizon merge to form the Schwarzschild horizon [10].

TABLE 1. VELOCITY IN DIFFERENT COORDINATE SYSTEMS [7].

		Schwarzschild	Gullstrand-Painlevé
Particles	Coordinate velocity: $\frac{dr}{dt}$, Proper velocity:$\frac{dr}{d\tau}$	$\pm(1 - \frac{2GM}{r})\sqrt{\frac{2GM}{r}}$, $\pm\sqrt{\frac{2GM}{r}}$	$-\sqrt{\frac{2GM}{r}}$, $\pm\sqrt{\frac{2GM}{r}}$
Light rays	Coordinate velocity:$\frac{dr}{dt}$	$\pm\left(1 - \frac{2GM}{r}\right)$	$\pm 1 - \sqrt{\frac{2GM}{r}}$

TABLE 2. SIX WIDELY USED FORMS OF THE SCHWARZSCHILD METRIC [7].

Schwarzschild metric in various coordinates	Coordinate transformation	Characteristic properties
Schwarzschild: $ds^2 = -(1 - \frac{2m}{r})dt^2 + \frac{1}{1-\frac{2m}{r}}dr^2 + r^2 d\Omega^2$	None	Area of spheres r = const is the 'Euchidean' $4\pi r^2$
Isotropic: $ds^2 = -(\frac{1-\frac{m}{2\bar{r}}}{1+\frac{m}{2\bar{r}}})^2 dt^2 + (1 + \frac{m}{2\bar{r}})^4(d\bar{r}^2 + \bar{r}^2 d\Omega^2)$	$r = \bar{r}(1 + \frac{m}{2\bar{r}})^2$	Constant-curvature time slices
Eddington-Finkelstein: $ds^2 = -(1 - \frac{2m}{r})dv^2 + 2dvdr + r^2 d\Omega^2$	$v = t + r + 2m\ln\left\|\frac{r}{2m} - 1\right\|$	Ingoing light rays: $dv = 0$
Kerr-Schild: $ds^2 = (\eta\alpha\beta + 2ml_a l_b)dx^\alpha dx^\beta$, $l_\alpha = \frac{1}{\sqrt{r}}(1, \frac{x}{\sqrt{r}}, \frac{y}{\sqrt{r}}, \frac{z}{\sqrt{r}})$	$\bar{t} = v - r$, $r^2 = x^2 + y^2 + z^2$	'Cartesian' coordinates
Lemaître: $ds^2 = dT^2 + \frac{2m}{r}dR^2 + r^2 d\Omega^2$, $r = [\frac{2\sqrt{2m}}{3}(R - T)]^{\frac{2}{3}}$	$dT = dt + \sqrt{\frac{2m}{r}}\frac{1}{1-\frac{2m}{r}}dt$ $dR = dt + \sqrt{\frac{r}{2m}}\frac{1}{1-\frac{2m}{r}}dr$	Infalling particles: $dR = 0$
Gullstrand-Painlevé: $ds^2 = -(1 -$	$dt = d\tilde{t} -$	Infalling particles: $dr =$

$\frac{2m}{r})d\tilde{t}^2 + 2\sqrt{\frac{2m}{r}}d\tilde{t}dr + dr^2 + r^2d\Omega^2$	$\frac{dt}{\sqrt{\frac{r}{2m}}-\sqrt{\frac{2m}{r}}}$	$-\sqrt{\frac{2m}{r}}d\tilde{t}$

TABLE 3. THE THREE CLASSICAL REPRESENTATION OF THE KERR METRIC [10].

Kerr-Schild$ds^2 = -dt^2 + dx^2 + dy^2 + dz^2 + \frac{2mr^2}{r^4+a^2z^2}(dt + \frac{r(xdx+ydy)}{a^2+r^2} + \frac{a(ydx-xdy)}{a^2+r^2} + \frac{z}{r}dz)^2$	$x^2 + y^2 + z^2 = r^2 + a^2(1 - \frac{z^2}{r^2}), r = r(x, y, z)$	$x = (r\cos\phi + a\sin\phi)\sin\theta,$ $y = (r\sin\phi - a\cos\phi)\sin\theta$ $z = r\cos\theta$
Boyer-Lindquist $ds^2 = -(1 - \frac{2mr}{\rho^2})dt^2 - \frac{4mra\sin^2\theta}{\rho^2}dtd\phi + \frac{\rho^2}{\Delta}dr^2 + \rho^2d\theta^2 + (r^2 + a^2 + \frac{2mra^2\sin^2\theta}{\rho^2})\sin^2\theta d\phi^2$	$\rho^2 = r^2 + a^2\cos^2\theta$ $\Delta = r^2 - 2mr + a^2 = (r - r_+)(r - r_-)$	$dv = dt + \frac{r^2+a^2}{\Delta}dr$ $d\varphi = d\phi + \frac{a}{\Delta}dr$
Kerr original $ds^2 = -(1 - \frac{2mr}{\rho^2})(dv - a\sin^2\theta d\varphi)^2 + 2(dv - a\sin^2\theta d\varphi)(dr - a\sin^2\theta d\varphi) + \rho^2(d\theta^2 + \sin^2\theta d\varphi^2)$	$r_{E\pm} = m \pm \sqrt{m^2 - a^2\cos^2\theta}$ $r_\pm = m \pm \sqrt{m^2 - a^2}$	None

TABLE 4. THE SPATIAL APPEARANCES AND RELATIONSHIPS OF THE KERR METRIC.

Outer	Ergosurface	$r_{E+} = m + \sqrt{m^2 - a^2\cos^2\theta}$
Event	Horizon	$r_+ = m + \sqrt{m^2 - a^2}$
Cauchy	Horizon	$r_- = m - \sqrt{m^2 - a^2}$
Inner	Ergosurface	$r_{E-} = m + \sqrt{m^2 - a^2\cos^2\theta}$
	singularity	$r = 0$

The Kerr-Newman black hole is a kind of charged rotating black hole with an angular momentum, whose geometry can be illustrated as following [11]:

$$ds^2 = \frac{\rho^2}{\Delta}dr^2 + \rho^2d\theta^2 + \frac{sin^2\theta}{\rho^2}[(r^2 + a^2)d\phi - acdt]^2 - \frac{\Delta}{\rho^2}[asin^2\theta d\phi - cdt]^2 \quad (13)$$

where,

$$\rho^2(r, \theta) = r^2 + a^2cos^2\theta \quad (14)$$

$$\Delta(r) = r^2 - 2Mr + a^2 + Q^2 + P^2 \quad (15)$$

and,

$$a = \frac{J}{mc} \quad (16)$$

Similar to the Reissner-Nordström black hole,

$$M = \frac{Gm}{c^2} \quad (17)$$

$$Q^2 = \frac{q^2G}{4\pi\varepsilon_0c^4} \quad (18)$$

The parameter P corresponds to the magnetic monopole, a is called the Kerr parameter. At the coordinate singularities Δ(r) = 0, the Kerr–Newman black hole spacetime has two horizons represented by radii r , where outer and inner horizons are r_+ and r_- [11].

$$r_{\pm} = M \pm \sqrt{M^2 - a^2 - Q^2 - P^2} \tag{19}$$

The inner and outer ergosphere is given by

$$r_{e_{\pm}} = M \pm \sqrt{M^2 - a^2 cos\theta - Q^2} \tag{20}$$

Figure 5 shows a charged rotating black hole with angular momentum J in spherical coordinates (r, ,). Figure 6 illustrates the inner structure of both Reissner–Nordström and Kerr–Newman black hole, where the near the origin of axis is the singularity ring, the area between singularity ring and the middle circle is the inner horizon, the area outside the inner horizon but inside the outermost circle is the outer horizon.

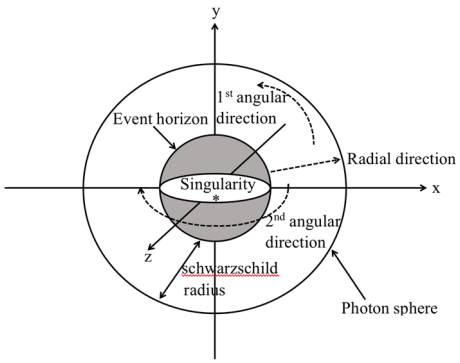

Figure 3. Anatomy of a Schwarzschild black hole.

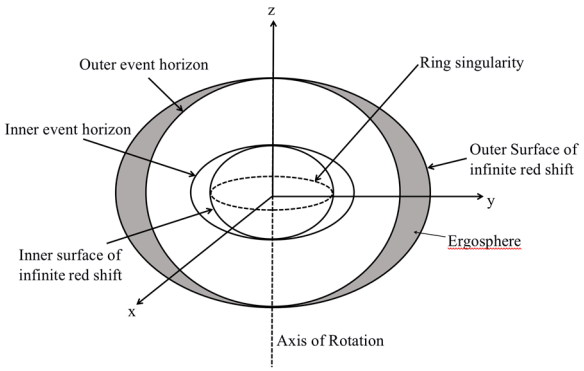

Figure 4. A sketch of Kerr black hole.

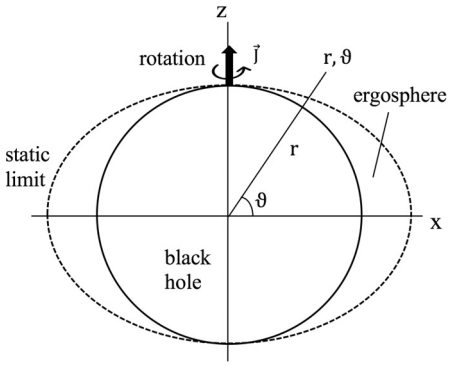

Figure 5. Kerr–Newman black hole [12].

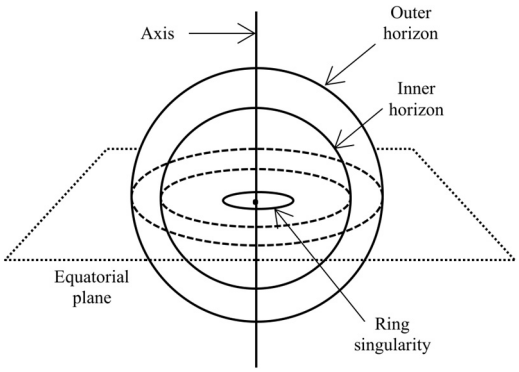

Figure 6. Structure of a charged black hole [13].

Table 5 lists the difference among these four types of black holes, the reference parameters are charge and angular momentum that describe whether the black hole is charged or uncharged and whether the black hole is rotated or not. The detail differences are demonstrated in Ref. [14].

TABLE 5. TABLE TYPE STYLES

	Non-rotating (J = 0)	Rotating (J > 0)
Uncharged (Q = 0)	Schwarzschild	Kerr
Charged (Q ≠ 0)	Reissner–Nordström	Kerr–Newman

4. DETECTION OF BLACK HOLE

4.1. Detector

For any physical theory's validity to be tested, experimental evidence certainly holds high credit. Thus, researchers have been reaching out for observations into the universe to learn more about the universe, and to modify current theory on the cosmos. In addition, it's quite obvious that specific detectors are needed for cosmological purpose. Intended for different intentions, detectors also various from one another, including ground-based ones and space-based ones, one's probes actively and that detect passively. Despite these differences, none of the detectors can be built without proper technology, location, and enough fund supported, in fact, several detectors who are competent in such large-scale observations includes LIGO, LISA, Virgo, KAGRA, Cosmic Explorer (CE), Einstein Telescope (ET), Tianqin, dark matter detectors DARWIN, ARGO, and DAMPE, neutrino detectors Hyper-Kamiokande, JUNO and DUNE, and also Chandra X-ray Observatory CXO. What's more, different network is also applied of certain detector, e.g., LIGO-Hanford (H), LIGO-Livingston (L), Hanford–Livingston–Virgo (HLV), Hanford–Livingston (HL), Hanford–Virgo (HV) and Livingston–Virgo (LV) [15]. With tench, as well as academic advancing, researchers have been trying to improve the instruments to allow for further observations, increasing in configurations, distances and precision than previously allowed.

4.2. Detection of black holes (electric charge)

The black hole charge can be determined by using the characteristic properties of gravitational retro-lensing images. The electromagnetic signal from a source located in front of a black hole may be significantly enhanced by the influence of strong gravitational lensing, this is the retro-lensing effect [16]. If we consider a photon with motion in the r-coordinate depends on the root multiplicity of the polynomial $\widehat{\mathrm{R}}(\hat{\mathrm{r}})$ that satisfies

$$\widehat{\mathrm{R}}(\hat{\mathrm{r}}) = \frac{R(r)}{M^4E^2} = \hat{r}^4 - \xi^2\hat{r}^2 + 2\xi^2\hat{r} - \hat{Q}^2\xi^2 \tag{21}$$

The critical value of the impact parameter for a photon to be captured by a Reissner–Nordström black hole depends on the multiplicity root condition of the polynomial R(r). Introducing the notation $\xi^2 = l$, $Q^2 = q$,

$$\mathrm{R(r)} = r^4 - lr^2 + 2lr - qr \tag{22}$$

Thus, one derives

$$\Delta = 16l^3[l^2(1-q) + l(-8q^2 + 36q - 27) - 16q^3] \tag{23}$$

where the polynomial R(r) should obey the following expression for roots to exist,

$$l^3[l^2(1-q) + l(m(q)) - 16q^3] = 0 \tag{24}$$

where $m(q) = 8q^2 - 36q + 27$. Thereby, one obtains the critical value of the impact parameter,

$$l = \frac{m(q) + \sqrt{m^2(q) + 64q^3(1-q)}}{2(1-q)} \tag{25}$$

The detail discussions for the solutions are given in Refs. [16, 17].

4.3. Measurement and estimation of mass

Twin-peak QPOs: Variations in the accretion flow surrounding compact objects, (e.g., white dwarfs, neutron stars, and black holes), are thought to cause quasi-periodic oscillations (QPOs). In high-frequency QPO oscillations, the inverse mass scaling theory can be used to determine the system's mass. The unknown mass (MH) can be measured by using the formular:

$$M_H = \left[v_{10}^{Hi} \Big/ v_H^{Hi} \right] \times 10M_\odot \tag{26}$$

where H stands for the quantities of the unknown system, and v_H^{Hi} is the higher peak value of the QPO frequency of an unknown object, M_H is unknown mass, $M_\odot$ is the solar mass, v_{10}^{Hi} is High-frequency QPO.

The number of unknown systems is represented by the subscript H, while the peak of the unknown object's QPO frequency is represented by v_H^{Hi}. Fig. 7. is used to calculate the v_{10}^{Hi} value of the $10M_\odot$ black hole. Two frequency curves are drawn based on the v_{10}^{Hi} peak ratio. The peak ratio between 1 and 2 is = 0.999 on the curve, and the lower curve (ratio between extreme peaks 2 and 1.35) is $\in (1, -1)$ short extension curve (straight line) =0.999 from the peak ratio between 1.35 and 1. The v_H^{Hi} frequency and ratio are used to describe the positions of different microquasars. A point can be determined on these curves to acquire the unknown frequency v_{10}^{Hi} of a $10M_\odot$ candidate black hole using peak correlation ratio knowledge. The mass is computed this way using a formular.

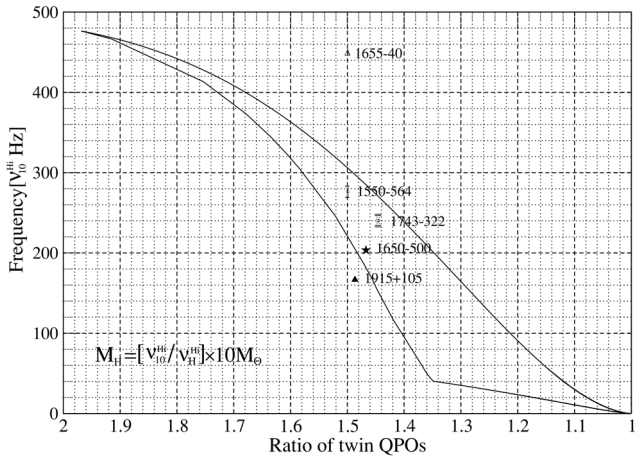

Figure 7. The peak ratios of a 10 M black hole's high-frequency (v_{10}^{Hi}) QPO are displayed versus their peak ratios [17].

As for accretion disks method, a flux variation from a point-like central source reaching a distant observer at time t_0 will be echoed after a span of time $\mathrm{t}-\mathrm{t}_0$ by the disc region created by omitting any general relativistic delays in light transmission.

$$t - t_0 = r(1 - sini \times sin\phi)/c \tag{27}$$

where I is the inclination angle from which the disk is observed. The highest blueshifts and redshifts in the echo front are produced in the weak-field approximation ($\mathrm{r} \gg \mathrm{r_s}$).

$$sin\phi_f = \{(sini)^{-1} - [(sini)^{-2} + 3]^{1/2}\}/3 \tag{28}$$

Where ϕ_f is the corresponding coordinate in the the disk plane.

$$r_f = c(t - t_0)\left(1 - sin\phi_f sini\right)^{-1} - r_s \tag{29}$$

Here, r_s is Schwarzschild radii, r_f is the corresponding radii, the last component on the right-hand side was added to roughly account for generic relativistic corrections at small radii:

$$(1+\mathrm{z})_\mathrm{f} = \left(1 - \frac{3\mathrm{r_s}^{-1/2}}{2\mathrm{r_f}}\right)\left\{1 \pm \frac{\cos\beta_\mathrm{f}}{[2\mathrm{r_f}(1+\tan^2\xi_\mathrm{f})/\mathrm{r_s} - 2]^{1/2}}\right\} \tag{30}$$

Where $(1+\mathrm{z})_\mathrm{f}$ is the shifts of the drifting features, $cos\beta_f = cos\phi_f sini(1 - sin^2\phi_r sin^2 i)^{-1/2}$ and $\tan\xi_\mathrm{f} = \tan\phi_\mathrm{f}\cos\beta_\mathrm{f}$. Over a broad range of disc settings, the drifting features' shifts $(1+\mathrm{z})_\mathrm{f}$ are accurate to a few percent [18].

In Fig. 8, the solid line depicts our best power law fit for the data, whereas the dotted line depicts the thin disc theory's projected findings [19]. The predicted variance owing to the tendency is shown by the shadow band around the best fit. The solid line at the bottom of the illustration represents the tolerable radius range of the accretion disk's inner edge, representing stable circular orbits of the innermost layers of the greatest revolving Kerr black hole and Schwarzschild black hole.

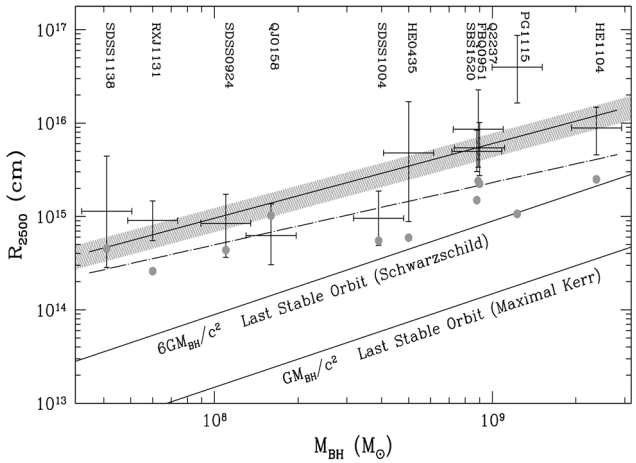

Figure 8. R_{250} accretion disc size corrected for inclination vs M_{BH} black hole mass [19].

4.4. Measurement and estimation of spin

QPOs (quasi-periodic oscillations) is a phenomenon that celestial body flickers at a particular frequency under the X-ray light range. Scholars gave the model of the QPOs of a black hole's system. As the reason for viscosity, the accretion flow is subsonic in the far distance and the position after the shock position while supersonic near the horizon. The oscillation shocks might be the reason of the QPOs [20]. As the double peak QPOs had been observed by X-ray variability of neutron stars, the models of resonance between epicyclic frequencies were made. Scholars have realized the orbit resonance and the ratio of the Quasi-periodic oscillation can help to solve questions about measurement of black hole's spin and others. The relationship of the Keplerian and epicyclic frequencies [21]. ν_{vert} and ν_{rad} with mass M and parameter about the spin a:

$$\nu_K = \frac{1}{2\pi}\left(\frac{GM_0}{r_G^3}\right)^{\frac{1}{2}}\left(x^{\frac{3}{2}} + a\right)^{-1} \tag{31}$$

$$\nu_{vert}^2 = \nu_K^2\left(1 - 4ax^{\frac{-3}{2}} + 3a^2x^{-2}\right) \tag{32}$$

$$\nu_{rad}^2 = \nu_K^2\left(1 - 6x^1 + 8ax^{\frac{-3}{2}} - 3a^2x^{-2}\right) \tag{33}$$

where ν_{rad} is radial epicyclic frequency, and x can be determined as $x = \frac{c^2 r}{GM}$. Those different types of resonance can help to get the formula of spin. The resonance constant could be $n{:}\,m$, which means:

$$n\nu_{rad} = m\nu \tag{34}$$

where ν can be the vertical orbital frequency or the Kepler frequency, and m,n are thought to be positive integers. For observed resonance number, the spin a can be calculated with a known mass and frequencies. As illustrated in Fig.9, the Török concluded that for the measurement of spin of Sgr A* showed the ratio of 3:2:1. By using 3:2 parametric resonance model, he gave the prediction about the spin range of Sgr A*, despite the 3:2 data is needed to be further confirmed.

Based on Fe-Kα line, a rotating black hole's Innermost stable circular orbit can be determined as [22]:

$$r_{isco} = \frac{GM}{c^2}\left[3 + \alpha + \sqrt{(3-\beta)(3+\beta+2\alpha)}\right] \tag{35}$$

Where

$$\begin{cases} \alpha = \sqrt{3\tau^2 + \beta} \\ \beta = 1 + \sqrt[3]{1-\tau^2}\left(\sqrt[3]{1-\tau} + \sqrt[3]{1+\tau}\right) \\ \tau = \dfrac{cJ}{M^2G} \end{cases} \tag{36}$$

If the accretion disk flows through the innermost stable circular orbit, it will make the innermost circular (ISCO) detected (seen from Fig.10 [23]). Inside the ISCO, the X-ray radiation cannot be observed since the accretion material that can be ionized is relative rare compared to outside of the ISCO. The Fe − Kα line is the most remarkable emission line which can be detected outside the ISCO, and the Fe − Kα line can gave us the details about the range of ISCO. For example, XTE JI550-546, was measured by this method, getting the result of the parameter $a \approx 0 \cdot 55^{+0.15}_{-0.22}$ [24].

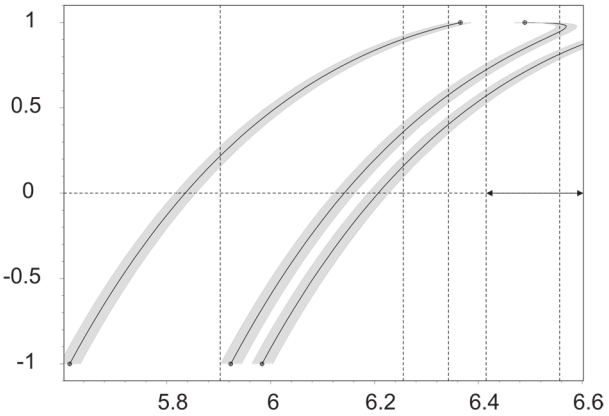

Figure 9. The relation for spin parameter a and $log(M\,/\,M_{\odot})$ when the resonance constant be 3:2 parametric, 3:1 and 2:1 for Sgr A*, and the shadows represent the degree of uncertainty [21].

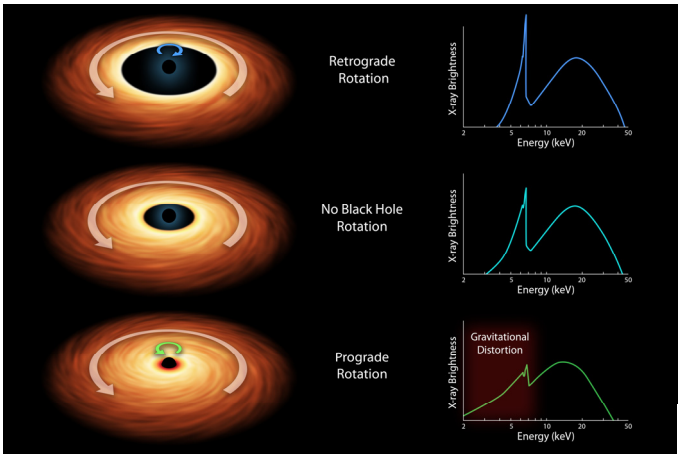

Figure 10. The X-ray's brightness distribution under different energy for retrograde rotation black holes, non-rotating black holes and prograde rotating black holes [23].

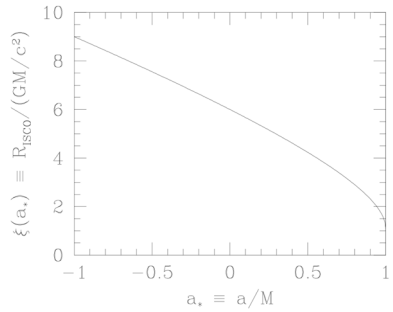

Figure 11. The dependence of $\frac{R_{isco}}{GM/c^2}$ on the spin parameter a_* [27].

Regarding to continuum fitting method, it includes analyzing the data from the thermal continuum spectrum of the black holes' accretion disk and fitting with theoretical models. According to the model of thin accretion disc black holes developed by Novikov and Thorne which they improved from Shakura and Sunyaev's model, one can get the expression of the R_{isco} with the thermal spectrum parameters [24].

$$\frac{3GM\dot{M}}{8\pi R^3}\left(1-\sqrt{\frac{R_{isco}}{R}}\right)=\sigma T_{eff}^4(R) \tag{37}$$

$$T_{eff}(R)=T^*\left(\frac{R_{isco}}{R}\right)^{\frac{3}{4}}\left(1-\sqrt{\frac{R_{isco}}{R}}\right)^{\frac{1}{4}} \tag{38}$$

Here, T_{eff} is the effective temperature related to the black body radiation, as the accretion disk's similarity with the black body. σ is the Stefan-Boltzmann constant. With given geometric parameters, by analyzing the data from the emission spectrum of it, researchers can get the R_{isco}. Furthermore, as shown in Fig.11, researchers can produce the spin parameter a by its monotone relation with $\frac{R_{isco}}{M}$ [26, 27]. Some researchers have discussed about the deviation of the disc model developed by Novikov and Thorne. As a reason of the model using an extreme thin accretion disc model, the deviation of spin parameter a may reach 0.2 when the accretion disk thickness parameter $\frac{h}{r}\sim 0.04-0.08$ [28].

Therefore, the condition for using the Novikov-Thorne model is the optically and geometrically thin of the disc.

5. LIMITATION AND FUTURE PROSPECT

When applying the twin-peak QPOs theory for measuring the mass, the relation between 'frequency' and 'ratio of twin QPOs' is plotted in Fig. 7 so that the unknown frequency can be derived. Yet, the curve itself is a modified one to be smooth, which could lead to a certain degree of inaccuracy. Additionally, as the QPOs theory suggests, the mass we get using the tangent line, relevant formation is the smallest possible mass of micro quasars rather than the practical one. As for the accretion desk method, apart from the certain condition needed to fit the weak-field approximation, this method is also currently restricted to certain types of black holes including Schwarzschild and Kerr ones. When making use of quasi-periodic oscillations to measure the spin, the mass should be calculated as a previous step, thus allow the possibility of accumulated error. Moreover, as mentioned above, the 3:2 data applied here need further confirmation. As apropos of continuum fitting method, disc has to be optically and geometrically thin, and this sets a limit the spin detectable under this circumstance. When it comes to detecting electric charge, type of black hole observable is also limited.

For future observation to hold more exactitude and farther space allowed, the possibility lies in more advanced instruments supported by improved technique as well as other theories discovered allowing less error and more types of black hole to be observed.

6. CONCLUSION

In conclusion, this paper investigates characteristic of different types of black holes and measurements of the three parameters of black holes. We study the four types of black holes (Schwarzschild black hole, Reissner-Nordström black hole, Kerr black hole, Kerr-Newman black hole) and demonstrates the space time metrics behind it. We mainly discuss about the measurements of the spin, mass and charge of a black holes. Specifically, the state-of-art detectors which made effort in detecting black holes are demonstrated. For the measurement of the mass, twin peaks QPOs and accretion disks methods are introduced. For the measurement of the spin, we discussed about double peaks QPOs method, the Fe-Kα line and Continuum fitting method. For the measurement of electric charge, the characteristic properties of gravitational retro-lensing images are mentioned. The limitations of those methods are discussed, similar to the inaccuracy and the selective black holes types from the twin-peak quasi-periodic oscillations method, the model limitation for long term continuum etc. According to the analysis, one can raise the prospect of higher accuracy detection with coming instruments and advanced theories. Overall, these results offer a guideline of detection for black holes.

REFERENCES

[1] B. Brügmann, A. Ghez, J. Greiner, J, "Black holes," Proceedings of the National Academy of Sciences, vol. 98(19), 2001, pp.10525-10526.
[2] B. Willke, "Observation of gravitational waves from a binary black hole merger – dawn of a new astronomy," Symmetry: Culture and Science, vol. 29(2), 2018, pp.257-264.
[3] M. Visser, "The Kerr spacetime: A brief introduction," arXiv preprint arXiv:0706.0622, 2007.
[4] B. Carr, et al., "Constraints on primordial black holes," Reports on Progress in Physics, vol. 84(11), 2021, 116902.
[5] A. Chael, et al., "The role of electron heating physics in images and variability of the Galactic Centre black hole Sagittarius A," Monthly Notices of the Royal Astronomical Society, vol. 478(4), 2018, pp. 5209-5229.
[6] M. Zajaček, et al, "Constraining the charge of the Galactic centre black hole," Journal of Physics: Conference Series, Vol. 1258, No. 1, 2019, pp. 012031, IOP Publishing.
[7] K. V. Kuchař, "Geometrodynamics of Schwarzschild black holes." Physical Review D, vol. 50.6, 1994, 3961.

[8] A. Hamilton, J. Lisle, "The river model of black holes." American Journal of Physics, vol. 76(6), 2008, pp.519-532.
[9] I. Petkov, "The Kerr Metric of Spinning Black Holes,", 2015 (), available at: https://www.researchgate.net/publication/276857998
[10] C. Heinicke, F. Hehl, "The Schwarzschild black hole," The Galactic Black Hole, vol. 12, 2002, pp. 3–34.
[11] H, Vargas-Rodríguez, et al., "Types of electromagnetic fields around black holes in Schwarzschild, Kerr and Kerr-Newmann spacetimes," arXiv preprint arXiv:2202.11707, 2022.
[12] Retrieving from: https://astronuclphysics.info/Gravitace4-4.htm
[13] Retrieving from: https://www.researchgate.net/figure/Sketch-of-a-Kerr-black-hole-with-its-two-horizons-and-the-ring-singulatrity_fig2_265603056
[14] Retrieving from: https://heasarc.gsfc.nasa.gov/docs/objects/heapow/archive/compact_objects/spinning_bh_chandra.html
[15] C. Cahillane, G. Mansell, "Review of the Advanced LIGO gravitational wave observatories leading to observing run four," Galaxies, vol. 10(1), 2022, 36.
[16] A. Zakharov, et al., "Direct measurements of black hole charge with future astrometrical missions," Astronomy & Astrophysics, vol. 442(3), 2018, pp.795-799.
[17] S. Mondal, "Black Hole Mass and Spin from the 2: 3 Twin-peak QPOs in Microquasars," The Astrophysical Journal, vol. 708(2), 2009, 1442.
[18] L. Stella, "Measuring black hole mass through variable line profiles from accretion disks," Nature, vol. 344(6268), 1990, pp. 747-749.
[19] C. W. Morgan, et al., "THE QUASAR ACCRETION DISK SIZE-BLACK HOLE MASS RELATION," The Astrophysical Journal, vol. 712(2), 2010, pp. 1129–1136.
[20] S. Mondal, "October. Estimation of spin of the black hole from QPO frequency," In AIP Conference Proceedings Vol. 1053, No. 1, 2008, pp. 349-352, American Institute of Physics.
[21] G. Török, "QPOs in microquasars and Sgr A.: measuring the black hole spin," Astronomische Nachrichten: Astronomical Notes, vol. 326(9), 2005, pp. 856-860.
[22] J. M. Bardeen, W. H. Press, S. A. Teukolsky, "Rotating black holes: locally nonrotating frames, energy extraction, and scalar synchrotron radiation," The Astrophysical Journal, vol. 178, 1972, pp. 347-370.
[23] Retrieving from: https://photojournal.jpl.nasa.gov/catalog/PIA16696
[24] J. F. Steiner, et al. "The spin of the black hole microquasar XTE J1550−564 via the continuum-fitting and Fe-line methods," Monthly Notices of the Royal Astronomical Society, vol. 416(2), 2011, pp. 941-958.
[25] I. D. Novikov, K. S. Thorne, "Astrophysics of black holes," In Black holes, 1973.
[26] S. L Shapiro, S. A. Teukolsky, "Black holes, white dwarfs, and neutron stars: The physics of compact objects," John Wiley & Sons, 2008..
[27] Shafee, R., McClintock, J. E., Narayan, R., Davis, S. W., Li, L. X., & Remillard, R. A. (2005). Estimating the spin of stellar-mass black holes by spectral fitting of the X-ray continuum. The Astrophysical Journal, 636(2), L113.
[28] A. K. Kulkarni, et al., "Measuring black hole spin by the continuum-fitting method: effect of deviations from the Novikov–Thorne disc model," Monthly Notices of the Royal Astronomical Society, vol. 414(2), 2011, pp. 1183-1194.